

Band gap Green's functions and localized oscillations

Alexander B Movchan and Leonid I Slepyan

Proc. R. Soc. A 2007 **463**, 2709-2727

doi: 10.1098/rspa.2007.0007

References

This article cites 19 articles, 1 of which can be accessed free

<http://rspa.royalsocietypublishing.org/content/463/2086/2709.full.html#ref-list-1>

Article cited in:

<http://rspa.royalsocietypublishing.org/content/463/2086/2709.full.html#related-urls>

Email alerting service

Receive free email alerts when new articles cite this article - sign up in the box at the top right-hand corner of the article or click [here](#)

To subscribe to *Proc. R. Soc. A* go to: <http://rspa.royalsocietypublishing.org/subscriptions>

Band gap Green's functions and localized oscillations

BY ALEXANDER B. MOVCHAN^{1,*} AND LEONID I. SLEPYAN²

¹*Department of Mathematical Sciences, University of Liverpool,
Liverpool L69 7ZX, UK*

²*Department of Solid Mechanics, Materials and Systems,
Tel Aviv University, Tel Aviv 69978, Israel*

We consider some typical continuous and discrete models of structures possessing band gaps, and analyse the localized oscillation modes. General considerations show that such modes can exist at any frequency within the band gap provided an admissible local mass variation is made. In particular, we show that the upper bound of the sinusoidal wave frequency exists in a non-local interaction homogeneous waveguide, and we construct a localized mode existing there at high frequencies. The localized modes are introduced via the Green's functions for the corresponding uniform systems. We construct such functions and, in particular, present asymptotic expressions of the band gap anisotropic Green's function for the two-dimensional square lattice. The emphasis is made on the notion of the depth of band gap and evaluation of the rate of localization of the vibration modes. Detailed analysis of the extremal localization is conducted. In particular, this concerns an algorithm of a 'neutral' perturbation where the total mass of a complex central cell is not changed

Keywords: waves in lattice structures; localized defect modes; Green's functions

1. Introduction

The localized defect modes occur naturally in photonic crystal structures, as described by Poulton *et al.* (2003). Although the 'localized Green's functions' can be represented in the series form for a continuum system involving a doubly periodic array of circular inclusions, the analytical analysis of the solution is not feasible in this case and the numerical treatment is required for evaluation of the defect states. The aim of the present work is to develop a fully analytical framework for analysis of localized vibrations within certain classes of periodic structures. The periodic structures considered in this paper are simpler than those of Poulton *et al.* (2003); the band gap Green's functions are obtained in the simple analytical form. This leads to evaluation of the depth of a band gap and to solution of problems of optimal design for defect modes of extremal localization.

The classical topic of research on *Waves in Lattices* is well described in the monographs (Brillouin 1953; Maradudin *et al.* 1963). The substantial analysis of lattices with defects and applications in the solid-state physics are discussed in the

* Author for correspondence (abm@liv.ac.uk).

papers (Maradudin 1965; Mead 1973, 1996; Mead & Parthan 1979; Mead & Yaman 1991). Defect vibration modes in two-component chains were described in Bacon *et al.* (1962). The defect modes in the context of the theory of scattering of waves in solids were considered by Callaway (1964). Surface tension and surface modes in lattice structures are studied in Gazis & Wallis (1964). Certain types of lattice Green's functions in diatomic lattices were constructed by Morita & Horiguchi (1972). The recent developments in theoretical and experimental physics on the design of photonic crystal fibres have generated a substantial interest to the photonic (or phononic) band gap materials (John 1987; Yablonovitch 1987, 1993). Although most of the technological applications involve models of acoustics, electromagnetism or elasticity in continuous periodic structures, some of photonic crystal models based on 'mass-spring' lattices were also presented in Jensen (2003), Martinsson & Movchan (2003), Cai *et al.* (2005). Steady-state problems for free and forced non-resonant waves in lattices and continuous periodic structures were also considered in Langley (1996, 1997), Langley *et al.* (1997). Dynamic lattice Green's functions for frequencies within the pass bands were studied by Martin (2006). The star-shaped localized solutions in lattices are discussed in Slepyan & Ayzenberg-Stepanenko (submitted).

In the present paper, we address the issue of analytical representation and analysis for localized vibration modes within some continuous (including non-local elastic) and lattice structures. We also introduce the notion of the depth of the band gap characterizing the rate of decay of exponentially localized vibration modes. The structure of the paper is as follows.

Section 2 outlines general settings for the localized vibration modes within continuous or discrete structures. Section 3 addresses the issue of band gaps and hence localized vibration modes within continuous systems, including beams and rods on elastic foundations as well as non-local interaction elastic string. Localized vibration modes within uniform lattice structures are studied in §4, which includes explicit asymptotic representations for lattice Green's functions and estimates of the rate of decay of a general localized vibration mode. Section 5 deals with a complex lattice structure possessing band gaps for a certain range of frequencies. By introducing a mass perturbation within the central cell of the structure, we create a localized vibration mode, whose frequency and the rate of decay are related via a closed-form analytical representation. We determine the optimal frequency corresponding to the fastest decay of the localized vibration mode, and show the situations when such a localized mode can be created via a mass perturbation which does not change the overall mass of the central cell. Finally, in §6, some concluding remarks are given.

2. Some general considerations

Consider an infinite, uniform (continuous or discrete), scalar, linear, single dispersion branch system whose homogeneous Fourier-transformed equation is

$$[L(\mathbf{k}) - \Omega]u^F(\mathbf{k}) = 0, \quad (2.1)$$

where $\Omega = \omega^2$ is the frequency squared and the oscillating multiplier $\exp(i\omega t)$ is omitted. Note that for real \mathbf{k} , $L(\mathbf{k}) \geq 0$ for any stable system (possibly $L(0) = 0$ that reflects a free rigid displacement).

Assume there exists a stop band in Ω : $\Omega < \Omega_-$ or $\Omega > \Omega_+$, where no sinusoidal wave exist, that is, equation (2.1) has no non-trivial solution for real \mathbf{k} . This implies

$$L(\mathbf{k}) > \Omega_- \quad \text{or} \quad L(\mathbf{k}) < \Omega_+, \quad (2.2)$$

respectively.

Consider the Green's function for frequencies within these stop bands, for $x=0$, that is, the corresponding inverse transform, $u(0) = U$, of

$$u^{\text{F}}(\mathbf{k}) = \frac{1}{L(\mathbf{k}) - \Omega}. \quad (2.3)$$

It follows that

$$U > 0 \quad (\Omega < \Omega_-); \quad U < 0, \quad \Omega u^{\text{F}} < -1 \quad (\Omega > \Omega_+). \quad (2.4)$$

Now consider the same system without the external force but with a changed mass at the origin. Denoting the additional mass by M and using (2.1) we obtain

$$u^{\text{F}}(\mathbf{k}) = \frac{M\Omega U}{L(\mathbf{k}) - \Omega}. \quad (2.5)$$

The above equation and (2.3) imply that for a given $\Omega < \Omega_-$ there exists a localized waveform coincident with the Green's function, provided the additional mass is equal to

$$M = \frac{1}{\Omega U} \quad (2.6)$$

and the relations (2.4) yield

$$M > 0 \quad (\Omega < \Omega_-), \quad M < 0 \quad (\Omega > \Omega_+). \quad (2.7)$$

Thus, in the latter case, the mass increment appears to be negative. However, if this case concerns a discrete lattice (where the particle mass is taken as the mass unit) the total central mass, $1 + M$, appears to be positive. Indeed, referring to (2.4) we find that (n is the dimension of the system)

$$\Omega U = \frac{1}{(2\pi)^n} \int_{-\pi}^{\pi} \Omega u^{\text{F}}(\mathbf{k}) d\mathbf{k} < -1, \quad (2.8)$$

and hence $M > -1$.

These simple considerations are applicable to multiple vibration branch systems, at least for frequency regions adjacent to the band gap boundaries. Indeed, the frequency corresponding to any of the edges of the band gap is the resonant frequency and the displacement of a particle, where the Green's function force is applied, is infinitely large. Hence, in the corresponding neighbourhood, the displacement is large enough to support a localized mode due to the admissible variation of the mass, as stated in (2.6).

The examples considered in the sequel also show that the localized modes can be obtained within the entire band gap frequency interval via an admissible local perturbation of the waveguide.

3. Continuous systems

In this section, we discuss several examples of waveguides supporting localized vibration modes.

(a) *A beam on an elastic foundation*

From the equation

$$Du^{IV}(x) + (\kappa - \rho\Omega)u(x) = 0 \quad (D, \rho \text{ are constants}), \quad (3.1)$$

it follows that there is the lower bound for the sinusoidal wave frequency

$$\Omega_- = \kappa/\rho. \quad (3.2)$$

The Green's function for $0 < \Omega < \Omega_-$ is

$$u(x) = \frac{1}{8D\lambda^3} e^{-\lambda|x|} (\cos \lambda x + \sin \lambda|x|), \quad \lambda = \left(\frac{\kappa - \rho\Omega}{4D} \right)^{1/4}. \quad (3.3)$$

Thus, the localized mode exists for $\Omega < \kappa/\rho$ if a concentrated mass is attached to the beam. The mass–frequency relation is

$$M = \frac{1}{\rho\omega^2} \sqrt{8(\kappa - \rho\omega^2)^{3/4} D^{1/4}}. \quad (3.4)$$

(b) *A bending plate on an elastic foundation*

From the equation

$$D\Delta^2 u(x, y) + (\kappa - \rho\Omega)u(x, y) = 0, \quad (3.5)$$

it follows that there is the same lower bound as above for the sinusoidal wave frequency (3.2). The corresponding Green's function for the origin, $x=y=0$, is

$$u(0, 0) = \frac{1}{8\sqrt{D(\kappa - \rho\Omega)}}. \quad (3.6)$$

Thus, the corresponding concentrated mass is

$$M = \frac{8\sqrt{D(\kappa - \rho\Omega)}}{\rho\Omega}. \quad (3.7)$$

(c) *A string made of a non-local interaction material*

In the dispersion relation for a classical homogeneous material, $\Omega \rightarrow \infty$ as $k \rightarrow \pm \infty$; that is, there is no upper bound of the sinusoidal wave frequency. However, such a bound and hence a semi-infinite band gap can exist in the case of a non-local interaction material. We show this by a simplest example of a string. To this end, in the relation for the internal stress

$$\sigma = Eu'(x) = E\delta'(x) * u(x) = E\delta(x) * u'(x), \quad (3.8)$$

we replace the derivative of the delta function by a regular ‘pre-delta’ function; for this, we use the function

$$\begin{aligned} \delta_\alpha(x) &= \frac{\alpha}{2} e^{-\alpha|x|} \quad (\delta_\alpha(x) \rightarrow \delta(x) \text{ as } \alpha \rightarrow \infty), \\ \delta'_\alpha(x) &= -\frac{\alpha^2}{2} e^{-\alpha|x|} \text{sign } x \quad (\delta'_\alpha(x) \rightarrow \delta'(x) \text{ as } \alpha \rightarrow \infty). \end{aligned} \quad (3.9)$$

In terms of the Fourier transform,

$$[\delta_\alpha(x)]^F = \frac{\alpha^2}{\alpha^2 + k^2}, \quad [\delta'_\alpha(x)]^F = -\frac{\alpha^2 ik}{\alpha^2 + k^2}, \quad (3.10)$$

and instead of the Fourier transform of the oscillating string classical equation

$$[Eu'(x)]' + \varrho\Omega u(x) = 0, \quad (3.11)$$

for the constant modulus E and density ϱ , we obtain a new equation of the form

$$\left[\frac{E\alpha^2 k^2}{\alpha^2 + k^2} - \varrho\Omega \right] u^F(k) = 0. \quad (3.12)$$

The dispersion relation for this non-local interaction string has the upper bound $\Omega = \Omega_+ = c^2\alpha^2$, where $c = \sqrt{E/\varrho}$.

We now introduce the Green's function for this string as the displacement caused by the force term $\delta(x)$. For $\Omega > \Omega_+$, it is

$$u^F(k) = -\frac{k^2 + \alpha^2}{(\varrho\Omega - E\alpha^2)k^2 + \varrho\alpha^2\Omega}$$

$$u(x) = -\frac{1}{\varrho\Omega(1 - c^2\alpha^2/\Omega)} \left[\delta(x) - \frac{a^2 - \alpha^2}{a} e^{-a|x|} \right] \left(a = \frac{\alpha}{\sqrt{1 - c^2\alpha^2/\Omega}}, \quad \Omega > c^2\alpha^2 \right). \quad (3.13)$$

From this generalized solution, it follows that the additional mass density corresponding to the localized oscillations (3.13) is

$$M = -\varrho \left(1 - \frac{c^2\alpha^2}{\Omega} \right) > -\varrho \quad (x=0), \quad M + \rho > 0, \quad (3.14)$$

while the localization exponent is given by $\lambda = a$. The condition $\varrho + M > 0$ is satisfied if the external force term corresponding to the Green's function, $\delta(x)$ and hence the corresponding displacement (3.13) are replaced by

$$\delta(x) \rightarrow \delta(x) * H(b - |x|) = H(b - |x|), \quad u(x) \rightarrow u(x) * H(b - |x|), \quad \text{if } b \leq \frac{1}{2a}. \quad (3.15)$$

After such a regularization, with the admissible mass density change within the region $|x| < b$, the displacement function becomes regular.

Note that the upper bound of the frequency and the corresponding localized oscillation solution can also be introduced, in a similar way, for a beam made of a non-local interaction material. In this case, we can choose the corresponding pre-delta function whose Fourier transform is $\alpha^4/(\alpha^4 + k^4)$.

4. Uniform discrete systems

Next, we address localization effects within lattices of simple structure.

(a) *A discrete chain on a discrete elastic foundation*

We now use the following normalized variables: the particle mass, the bond stiffness and the cell size are taken as the natural units; the stiffness of the elastic foundation is denoted by κ . The equation in terms of the discrete Fourier transform is

$$[\kappa + 2(1 - \cos k) - \Omega]u^{\text{F}}(k) = 1. \quad (4.1)$$

There exist the upper and lower bounds for the sinusoidal wave frequency

$$\Omega_+ = 4 + \kappa \quad \text{and} \quad \Omega_- = \kappa. \quad (4.2)$$

For $\Omega > 4 + \kappa$,

$$u(m) = -\frac{2^{-|m|}}{\sqrt{(\Omega - \kappa)^2 - 4(\Omega - \kappa)}} \left(\sqrt{(\Omega - \kappa)^2 - 4(\Omega - \kappa)} - (\Omega - \kappa - 2) \right)^{|m|}, \quad (4.3)$$

and

$$M = \frac{1}{\Omega u(0)} = -\frac{\sqrt{(\Omega - \kappa)^2 - 4(\Omega - \kappa)}}{\Omega} \quad (\Omega > 4 + \kappa). \quad (4.4)$$

Thus, the localized oscillations exist for $\Omega > 4 + \kappa$ if one mass of the chain is lighter than the others, $0 < 1 + M < 1$.

For $0 < \Omega < \kappa$,

$$u(m) = \frac{2^{-|m|}}{\sqrt{(\kappa - \Omega)^2 + 4(\kappa - \Omega)}} \left(\kappa - \Omega + 2 - \sqrt{(\kappa - \Omega)^2 + 4(\kappa - \Omega)} \right)^{|m|} \quad (4.5)$$

and

$$M = \frac{1}{\Omega u(0)} = \frac{\sqrt{(\kappa - \Omega)^2 + 4(\kappa - \Omega)}}{\Omega} > 0 \quad (\Omega < \kappa). \quad (4.6)$$

Clearly, the latter gap does not exist for a free chain where $\kappa = 0$.

(b) *Localized Green's function for the square lattice*

Analysis of dynamic Green's functions for square lattices for frequencies within the pass band is given by [Martin \(2006\)](#). In this section, we address the case when the frequency of vibrations is outside the admissible pass band and hence when Green's function is exponentially localized.

Using the discrete Fourier transform from the equation for the square lattice, we find

$$u^{\text{FF}}(k, q) = \frac{1}{2(1 - \cos k) + 2(1 - \cos q) - \Omega}, \quad (4.7)$$

and

$$u(m, n) = \frac{1}{4\pi^2} \int_{-\pi}^{\pi} \int_{-\pi}^{\pi} \frac{\exp[-i(km + qn)]}{2(1 - \cos k) + 2(1 - \cos q) - \Omega} dk dq. \quad (4.8)$$

Successive integration leads to

$$\begin{aligned} u^F(k, n) &= \frac{1}{\pi} \int_0^{\pi} \frac{\cos qn dq}{2(1 - \cos k) + 2(1 - \cos q) - \Omega} \\ &= \frac{(-1)^{n+1}}{2\sqrt{a^2 - 1}} (a - \sqrt{a^2 - 1})^{|n|} \end{aligned} \quad (4.9)$$

$$a = \frac{\Omega}{2} - 2 + \cos k, \quad a > 1 \quad (\Omega > 8) \quad \text{and}$$

$$u(m, n) = \frac{(-1)^{n+1}}{\pi} \int_0^{\pi} \frac{1}{2\sqrt{a^2 - 1}} (a - \sqrt{a^2 - 1})^{|n|} \cos km dk. \quad (4.10)$$

Consider some particular cases.

(i) *Displacement at the origin* $m=n=0$

From (4.10), we have

$$u(0, 0) \sim -\frac{1}{2\sqrt{(\Omega/2 - 2)^2 - 1}}, \quad (\Omega \rightarrow \infty). \quad (4.11)$$

An exact and the asymptotic dependencies on Ω are presented in [figure 1](#). When $\Omega > 8$, the direct numerical computation shows that the asymptotic approximation (4.11) accurately represents the exact result (4.10). The graph of $u(0, 0)$ versus ω is shown in [figure 1](#).

(ii) *An asymptote for the bond-line rays*

For $m=0$, $n \rightarrow \infty$, we take into account the fact that asymptotically the main contribution corresponds to the integration in a small vicinity of $k=\pi$. So we represent

$$\cos k \sim -1 + (1/2)(\pi - k)^2, \quad (4.12)$$

$$a - \sqrt{a^2 - 1} \sim (c - \sqrt{c^2 - 1}) \left[1 - \frac{(\pi - k)^2}{2\sqrt{c^2 - 1}} \right], \quad c = \frac{\Omega}{2} - 3, \quad (4.13)$$

$$\left[1 - \frac{(\pi - k)^2}{2\sqrt{c^2 - 1}} \right]^{|n|} \sim \exp \left[-\frac{(\pi - k)^2 |n|}{2\sqrt{c^2 - 1}} \right] \quad \text{and} \quad (4.14)$$

$$u(0, n) \sim \frac{(-1)^{n+1}}{2\sqrt{c^2 - 1}} (c - \sqrt{c^2 - 1})^{|n|} \frac{1}{\pi} \int_{\pi-\epsilon}^{\pi} \exp \left[-\frac{(\pi - k)^2 |n|}{2\sqrt{c^2 - 1}} \right] dk, \quad (4.15)$$

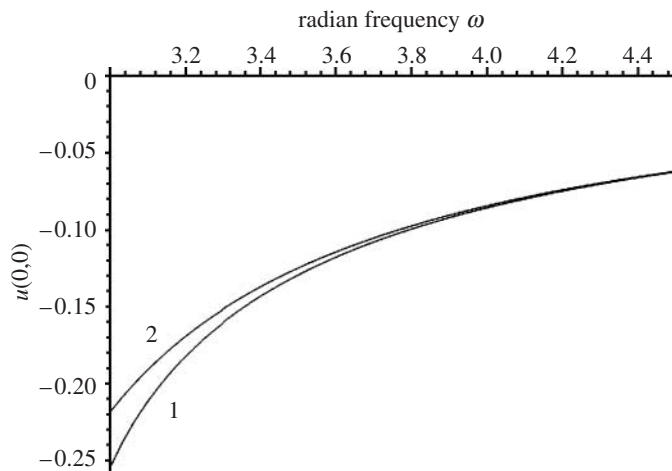


Figure 1. The value $u(0, 0)$ at the origin versus the radian frequency ω . (1) The exact result and (2) the asymptotic one (4.11).

for a small positive ε . Then

$$\frac{1}{\pi} \int_{\pi-\varepsilon}^{\pi} \exp\left[-\frac{(\pi-k)^2|n|}{2\sqrt{c^2-1}}\right] dk \sim \sqrt{\frac{2\sqrt{c^2-1}}{|n|}} \frac{1}{\pi} \int_0^{\infty} e^{-x^2} dx = \sqrt{\frac{\sqrt{c^2-1}}{2\pi|n|}} \quad (4.16)$$

and,

$$u(0, n) \sim \frac{(-1)^{n+1}}{\sqrt{8\pi\sqrt{c^2-1}}} \left(c - \sqrt{c^2-1}\right)^{|n|} \frac{1}{\sqrt{|n|}} \quad (n \rightarrow \infty). \quad (4.17)$$

The result is illustrated in figure 2. Owing to the symmetry, the same asymptote (with the change n to m) is valid for $u(m, 0)$.

(iii) *The asymptote for the diagonal rays $m = \pm n$*

For this case, it is useful to transform the integration domain \mathcal{A}_1 in (4.8) by adding four triangles to form a larger square, domain \mathcal{A}_2 with vertices on the k, q lines. Owing to 2π periodicity of the integrand, the integration over the latter domain, whose area is twice as much as the \mathcal{A}_1 area, results in $2u(m, n)$. Substituting

$$k = x + y, \quad q = x - y, \quad (4.18)$$

and taking into account that the \mathcal{A}_2 area on the (x, y) plane is equal to the \mathcal{A}_1 area, we get for $m = n$

$$u(m, m) = -\frac{1}{\pi^2} \int_0^{\pi} \int_0^{\pi} \frac{\cos 2mx}{\Omega - 4 + 4 \cos x \cos y} dx dy. \quad (4.19)$$

In the integral with respect to x , only small neighbourhoods of $y=0$ and $y=\pi$ are important for large m , and these neighbourhoods give equal leading contributions. So we can use one of the representations $\cos y \sim 1 - \frac{1}{2}y^2 (y \rightarrow 0)$

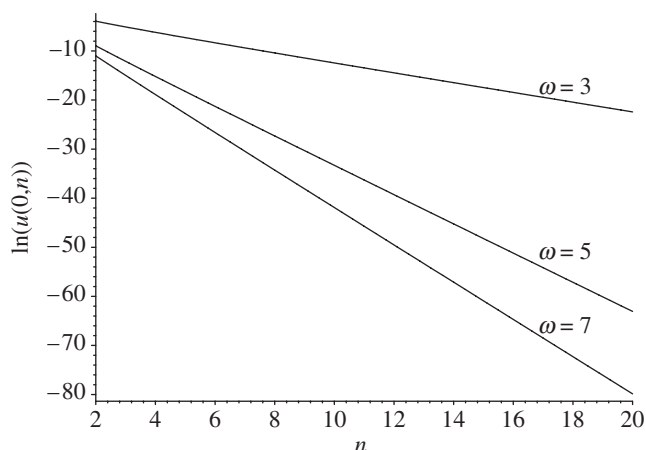


Figure 2. Asymptotic approximation of $\ln(u(0, n))$ versus n for different values of ω .

or $\cos y \sim -1 + \frac{1}{2}(\pi - y^2)(y \rightarrow \pi)$. Thus, we find that

$$\begin{aligned} u(m, m) &\sim -\frac{2}{\pi} \int_0^\infty \left[\frac{1}{\pi} \int_0^\pi \frac{\cos 2mx}{\Omega - 4 + 4(1 - y^2/2)\cos x} dx \right] dy \\ &\sim -\frac{1}{\sqrt{\Omega^2 - 8\Omega}} \frac{2}{\pi} \int_0^\infty \left(\frac{\sqrt{1 - b^2} - 1}{b} \right)^{2|m|} dy, \quad b = \frac{4(1 - y^2/2)}{\Omega - 4}. \end{aligned} \quad (4.20)$$

Further,

$$\begin{aligned} \left(\frac{\sqrt{1 - b^2} - 1}{b} \right)^{2|m|} &\sim \left(\frac{\sqrt{1 - b_0^2} - 1}{b_0} \right)^{2|m|} \left(1 - \frac{y^2}{2\sqrt{1 - b_0^2}} \right)^{2|m|} \\ &\sim \left(\frac{\sqrt{1 - b_0^2} - 1}{b_0} \right)^{2|m|} \exp\left(-\frac{|m|y^2}{\sqrt{1 - b_0^2}} \right), \quad b_0 = \frac{4}{\Omega - 4}. \end{aligned} \quad (4.21)$$

As a result,

$$u(m, m) \sim -\frac{1}{\sqrt{\pi}\sqrt{\Omega^2 - 8\Omega}} \left(\frac{\sqrt{1 - b_0^2} - 1}{b_0} \right)^{2|m|} \sqrt{\frac{\sqrt{1 - b_0^2}}{|m|}}. \quad (4.22)$$

In terms of the distance r from the origin, this relation looks as

$$u(m, m) \sim -\frac{1}{\sqrt{\pi}\sqrt{\Omega^2 - 8\Omega}} \left(\frac{\sqrt{1 - b_0^2} - 1}{b_0} \right)^{r\sqrt{2}} \sqrt{\frac{\sqrt{2(1 - b_0^2)}}{r}}. \quad (4.23)$$

Note that this result is valid for the lattice diagonal nodes only, that is for integer $m = n = r/\sqrt{2} \rightarrow \infty$.

(iv) *Localization exponent*

The functions

$$\begin{aligned}\lambda_{0n} &= c - \sqrt{c^2 - 1} = \Omega/2 - 3 - \sqrt{(\Omega/2 - 3)^2 - 1}, \\ \lambda_{mm} &= \left(\frac{\sqrt{1 - b_0^2} - 1}{b_0} \right)^{\sqrt{2}} = \left(\Omega/4 - 1 - \sqrt{(\Omega/4 - 1)^2 - 1} \right)^{\sqrt{2}},\end{aligned}\quad (4.24)$$

can be considered as the localization measures. The logarithmic derivative of the displacement with respect to the distance from the origin is asymptotically equal to λ , and hence λ is said to be the localization exponent. The quantities λ_{0n} and λ_{mm} are plotted as functions of the frequency in [figure 3](#). Their ratio is also presented. The results show that the localization increases as the frequency grows, and the oscillations are characterized by a more strong localization in the diagonal rays rather than in the bond-line rays. Numerical computations lead to the conclusion that these rays correspond to maximal and minimal localizations, respectively.

(c) *Exponential waves. Complex dispersion relation*

The dispersion equation for plane waves in the lattice has the form

$$\Omega = 4 - 2 \cos k_x - 2 \cos k_y. \quad (4.25)$$

When $\omega > \sqrt{8}$ this equation does not have real solutions, and we use the following substitution: $k_x = \pi + iq_x$, $k_y = \pi + iq_y$. Hence,

$$\Omega = 4 + 2 \cosh q_x + 2 \cosh q_y. \quad (4.26)$$

We seek the exponential wave, oriented in the n -direction ($q_x = 0$), in the form

$$u_0(n) = \exp(i\pi n - q_y n). \quad (4.27)$$

Hence, equation (4.26) implies

$$\exp(-q_y) = \lambda_{0n} = c - \sqrt{c^2 - 1}. \quad (4.28)$$

Hence, according to (4.13) and (4.17), the logarithmic derivative of the asymptote (4.17) of the lattice Green's function differs from that of the exponential wave only by a slow term $-(1/2)\ln n$.

A similar statement holds for the exponential waves for $q_x = q_y$ and the corresponding asymptote of the lattice Green's function (4.23) for $m = n$.

It is of interest to note that the dispersion contour for $\omega = 2$ is a square ([figure 4a](#)) whose vertices belong to the coordinate axes. In other words, when ω is close to 2, the directions of the group velocity coincide with one of the diagonal lines $k_x = \pm k_y$. In contrast, for sufficiently large ω ($\omega > \sqrt{8}$) the corresponding

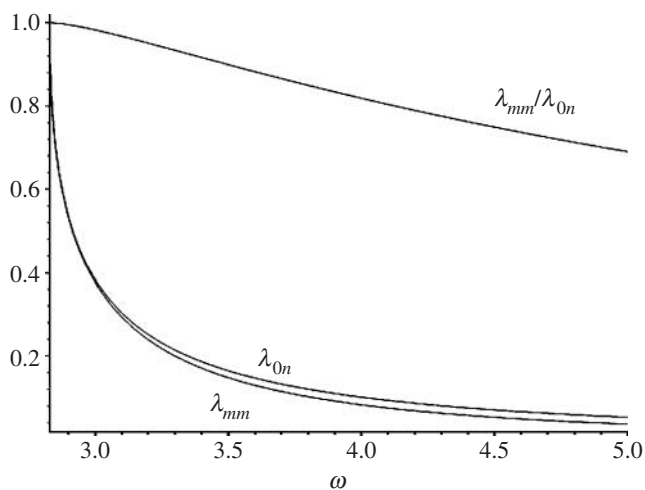


Figure 3. The quantities λ_{0n} , λ_{mm} as well as their ratio $\lambda_{mm}/\lambda_{0n}$ are plotted as functions of ω .

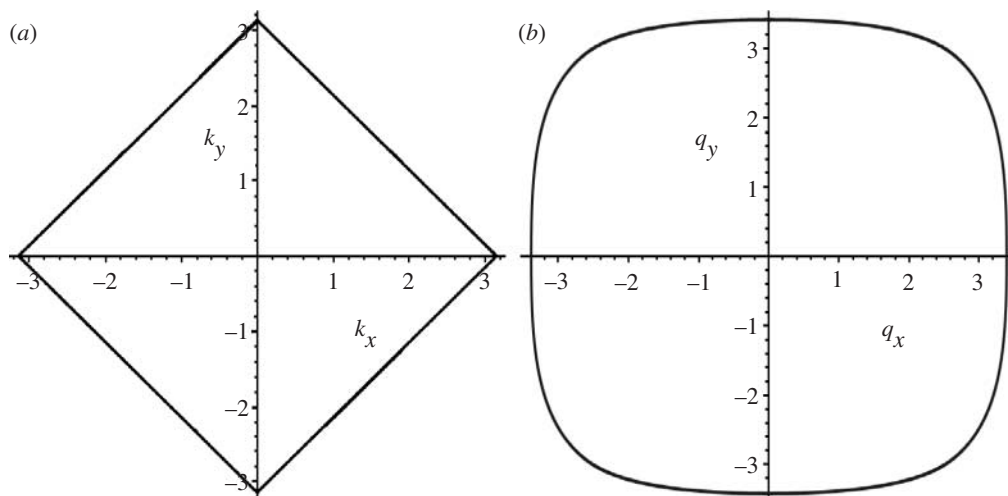


Figure 4. Dispersion contours: (a) the sinusoidal wave contour, $\omega=2$ and (b) the exponential wave contour, $\omega=6$.

dispersion contour, in the (q_x, q_y) plane, becomes close to a square whose sides are aligned with the coordinate axes (figure 4b).

5. Discrete system of a complex structure

Consider a two-mass chain shown in figure 5. The homogeneous dynamic equations are

$$m_1 \ddot{u}_{1,m} = u_{2,m} + u_{2,m-1} - 2u_{1,m} \quad \text{and} \quad m_2 \ddot{u}_{2,m} = u_{1,m} + u_{1,m+1} - 2u_{2,m}. \quad (5.1)$$

For the wave

$$u_{1,m} = u_{1,0} e^{ikm}, \quad u_{2,m} = u_{2,0} e^{ikm}, \quad (5.2)$$

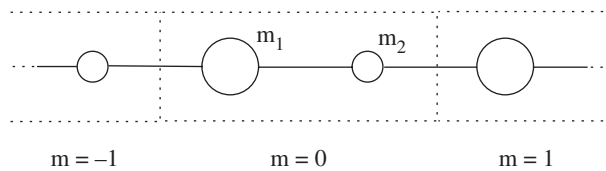


Figure 5. A two-mass chain.

the dispersion relation is as follows:

$$\Omega = \frac{m_1 + m_2}{m_1 m_2} \pm \sqrt{\left(\frac{m_1 + m_2}{m_1 m_2}\right)^2 - \frac{4 \sin^2 k/2}{m_1 m_2}}. \quad (5.3)$$

Let m_1 be greater than m_2 . The dispersion relation defines the finite band gap as

$$\Omega_- = \frac{2}{m_1} < \Omega < \frac{2}{m_2} = \Omega_+, \quad (5.4)$$

and the infinite one as

$$\Omega > \frac{2}{m_1} + \frac{2}{m_2}. \quad (5.5)$$

Now consider the Green's matrix function for these band gaps based on the equations

$$\begin{aligned} -m_1 \Omega u_{1,m} &= u_{2,m} + u_{2,m-1} - 2u_{1,m} + P_1 \delta_{0,m} \quad \text{and} \\ -m_2 \Omega u_{2,m} &= u_{1,m} + u_{1,m+1} - 2u_{2,m} + P_2 \delta_{0,m}. \end{aligned} \quad (5.6)$$

The discrete Fourier transform leads to the solution

$$\begin{aligned} u_1^F &= \frac{1}{Q} [-P_1(m_2 \Omega - 2) + P_2(1 + e^{ik})], \\ u_2^F &= \frac{1}{Q} [-P_2(m_1 \Omega - 2) + P_1(1 + e^{-ik})] \quad \text{and} \\ Q &= (m_1 \Omega - 2)(m_2 \Omega - 2) - 2(1 + \cos k), \end{aligned} \quad (5.7)$$

where $Q < 0$ for the finite band gap and $Q > 0$ for the infinite one.

(a) *Localized vibration modes within the finite band gap*

The inverse Fourier transform gives

$$\begin{aligned} u_{1,m} &= -\frac{1}{\sqrt{Q_0^2 - 4Q_0}} \{[-P_1(m_2 \Omega - 2) + P_2] \lambda^{|m|} + P_2 \lambda^{|m-1|}\}, \\ u_{2,m} &= -\frac{1}{\sqrt{Q_0^2 - 4Q_0}} \{[-P_2(m_1 \Omega - 2) + P_1] \lambda^{|m|} + P_1 \lambda^{|m+1|}\} \quad \text{and} \\ \lambda &= \frac{1}{2} (\sqrt{Q_0^2 - 4Q_0} + Q_0 - 2) \quad \left(\frac{2}{m_1} < \Omega < \frac{2}{m_2} \right), \end{aligned} \quad (5.8)$$

where the localization exponent $\lambda < 0$ ($|\lambda| < 1$). In particular,

$$\begin{aligned} u_{1,0} &= \frac{P_1(m_2\Omega - 2) - (1/2)P_2\left(Q_0 + \sqrt{Q_0^2 - 4Q_0}\right)}{\sqrt{Q_0^2 - 4Q_0}}, \\ u_{2,0} &= \frac{P_2(m_1\Omega - 2) - (1/2)P_1\left(Q_0 + \sqrt{Q_0^2 - 4Q_0}\right)}{\sqrt{Q_0^2 - 4Q_0}} \quad \text{and} \\ Q_0 &= (m_1\Omega - 2)(m_2\Omega - 2) < 0 \quad \left(\frac{2}{m_1} < \Omega < \frac{2}{m_2}\right). \end{aligned} \quad (5.9)$$

The same but homogeneous solution representing the localized oscillations can be obtained from this system of equations if we put $P_1 = M_1\Omega u_1$, $P_2 = M_2\Omega u_2$, where $M_{1,2}$ are the additional masses attached to the corresponding masses in the cell $m=0$. We arrive at the condition of the existence of a non-trivial solution as

$$\begin{aligned} &\left(\sqrt{Q_0^2 - 4Q_0} - M_1\Omega(m_2\Omega - 2)\right)\left(\sqrt{Q_0^2 - 4Q_0} - M_2\Omega(m_1\Omega - 2)\right) \\ &- \frac{M_1M_2\omega^4}{4}\left(\sqrt{Q_0^2 - 4Q_0} + Q_0\right)^2 = 0 \quad \left(\frac{2}{m_1} < \Omega < \frac{2}{m_2}\right). \end{aligned} \quad (5.10)$$

In particular, the above equation implies that when $M_2=0$

$$\begin{aligned} M_1 &= -\frac{1}{\Omega}\sqrt{\frac{m_1\Omega - 2}{2 - m_2\Omega}}\sqrt{4 - Q_0} = -\frac{2}{\Omega(1+r)}\sqrt{\frac{r\Omega - 1 - r}{1 + r - \Omega}} \\ &\quad \times \sqrt{(1+r)^2 + (r\Omega - 1 - r)(1 + r - \Omega)}, \end{aligned} \quad (5.11)$$

and when $M_1=0$ we have

$$\begin{aligned} M_2 &= \frac{1}{\Omega(1+r)}\sqrt{\frac{2 - m_2\Omega}{m_1\Omega - 2}}\sqrt{4 - Q_0} \\ &= \frac{2}{\Omega(1+r)}\sqrt{\frac{1 + r - \Omega}{r\Omega - 1 - r}}\sqrt{(1+r)^2 + (r\Omega - 1 - r)(1 + r - \Omega)}. \end{aligned} \quad (5.12)$$

Here and below, the mass ratio is denoted by $r = m_1/m_2 > 1$, and the normalization is introduced in such a way that $m_1 + m_2 = 2$, so that the corresponding homogeneous lattice is the same as in §4. In these terms

$$Q_0 = 4\left(\frac{\Omega}{1+r} - 1\right)\left(\frac{r\Omega}{1+r} - 1\right). \quad (5.13)$$

The analytical formulae (5.11) and (5.12) suggest that a localized defect mode can be initiated by a small variation of one of the masses in the central cell. Namely, a localized mode will appear near the lower edge of the band gap, i.e. $\Omega \rightarrow 2m_1^{-1} + 0$, when $M_2=0$ and $M_1 \sim -C\sqrt{m_1\Omega - 2}$, with C being a positive constant. We note that the localized mode near the lower edge of the band gap cannot be created by a small variation of m_2 with $M_1=0$. In figure 6, we present

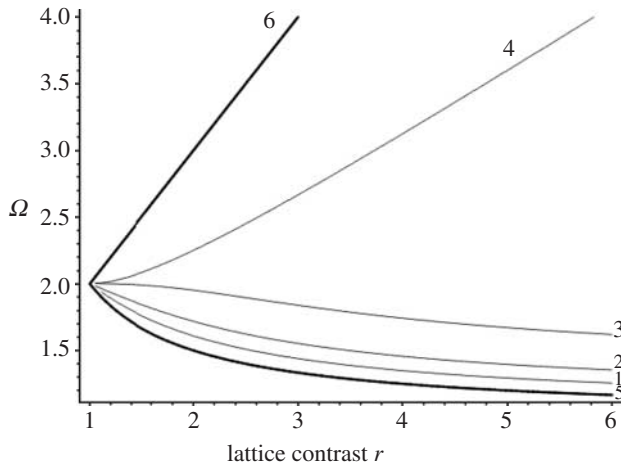


Figure 6. The frequency squared versus the lattice contrast for $M_2=0$. (1) $M_1 = -0.5$, (2) $M_1 = -0.7$, (3) $M_1 = -1$, (4) the limit curve $M_1 = -2r/(1+r)$, (5) the lower band gap boundary and (6) the upper band gap boundary.

the frequencies of the localized modes as functions of the mass ratio in the unperturbed biatomic lattice for the case when $M_2=0$ and M_1 is negative. This includes the curves corresponding to $M_1 = -0.5, -0.7, -1$, and the limit curve $M_1 = -2r/(1+r)$. In the latter limit case $m_1 + M_1 = 0$. Thus, the region between the limit curve and the lower edge of the band gap ($\Omega = 2/m_1 = 1 + 1/r$) can be covered via alteration of the mass m_1 while $M_1 + m_1 > 0$ and $M_2 = 0$. The band gap boundaries are also shown in figure 6.

In contrast, to obtain a localized vibration at the frequency close to the upper edge of the band gap, i.e. $\Omega \rightarrow 2m_2^{-1} - 0$, it is sufficient to increase the smaller mass m_2 , so that $M_2 \sim C\sqrt{2 - m_2\Omega}$, $C > 0$ while $M_1 = 0$. The localized mode near the upper edge of the band gap cannot be created by a small variation of m_1 while $M_2 = 0$. In figure 7, we show the frequencies of the localized modes as functions of the mass ratio $r = m_1/m_2$ for the case when $M_1 = 0$ and M_2 is positive. The diagram incorporates the curves corresponding to $M_2 = 0.5, 1, 2, 3$. The band gap region can be covered via increase of the mass m_2 while $M_1 = 0$. However, in order to reach the lower bound of the band gap, one has to take the limit as $m_2 \rightarrow +\infty$. Simultaneous finite variations of both masses m_1 and m_2 thus allow to create a localized mode over all the frequency range within the finite band gap.

(b) *The band gap depth and the extremal localization*

Within the band gap, $2m_1^{-1} < \Omega < 2m_2^{-1}$, the functions $u_{j,m}$, $j=1, 2$ decay exponentially as $|m|$ increases, and the localization exponent is equal to λ (see equation (5.8)). When $|\lambda|$ reaches its minimum within the gap as $\Omega = \Omega_*$, the oscillation region becomes most localized. These values are

$$|\lambda|_{\min} = \frac{1}{r} \left(\lambda = -\frac{1}{r} \right), \quad \Omega_* = \frac{1}{m_1} + \frac{1}{m_2} = 1 + \frac{1}{2} \left(r + \frac{1}{r} \right). \quad (5.14)$$

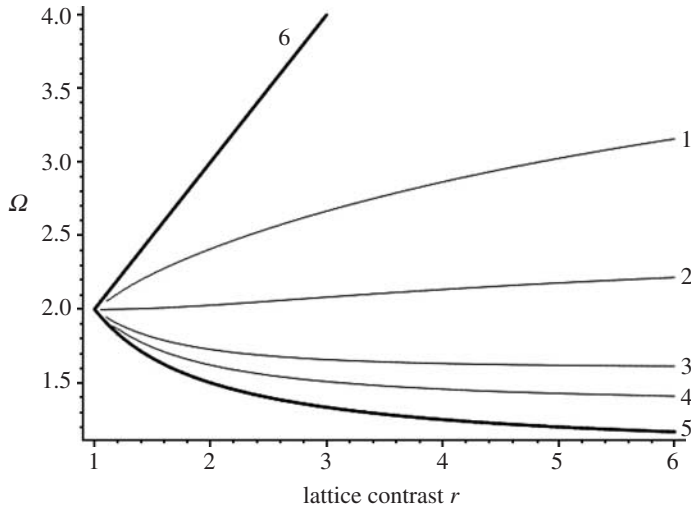


Figure 7. The frequency squared versus the lattice contrast for $M_1=0$. (1) $M_2=0.5$, (2) $M_2=2$, (3) $M_2=2$, (4) $M_2=3$, (5) the lower band gap boundary and (6) the upper band gap boundary.

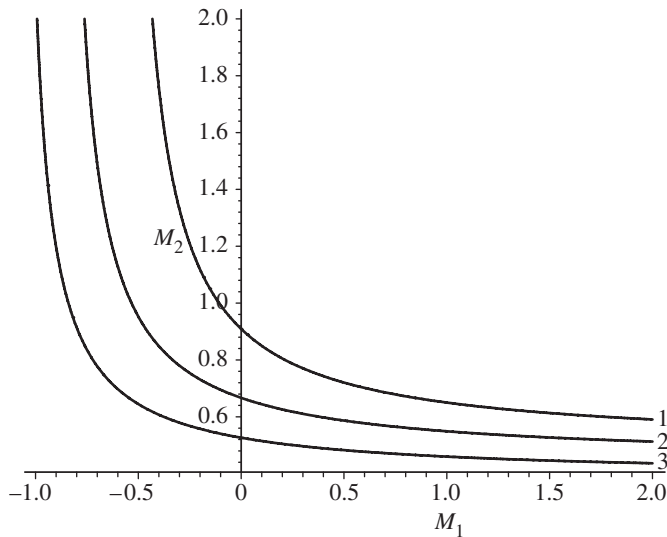


Figure 8. The perturbation mass M_2 versus M_1 for the case of extreme localization. Three cases of the lattice contrast are shown: (1) $r=1.2$, (2), $r=2$ and (3) $r=2.8$.

Assuming the normalization $m_1 + m_2 = 2$, we choose the perturbation masses M_1 and M_2 in such a way that the corresponding localized vibration has the extremal localization, with the localization exponent $\lambda = -1/r$. Figure 8 shows M_2 versus M_1 for the case of extremal localization, for the lattices of different contrasts. Three cases of the lattice contrast are presented ($r=1.2, 2, 2.8$). It is shown that for a fixed perturbation mass M_1 , the second perturbation mass M_2 decreases for a chain of a higher contrast. Figure 9 includes the graphs of the total perturbation mass $M_1 + M_2$ versus M_1 for the cases of the extremal localization

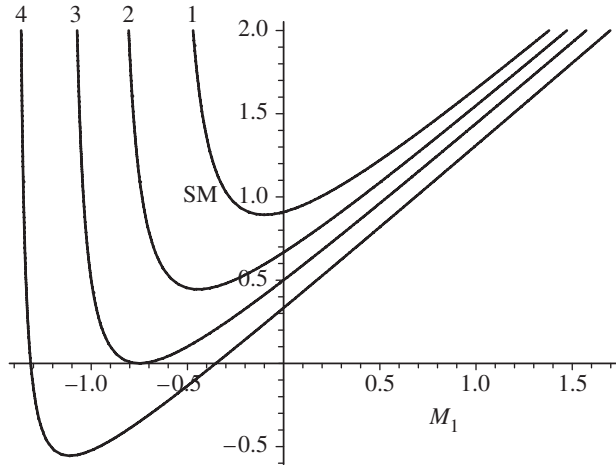


Figure 9. The total perturbation mass $M_1 + M_2$ versus M_1 for the case of the extremal localization for different lattice contrasts: (1) $r=1.2$, (2) $r=2$, (3) $r=3$ and (4) $r=5$.

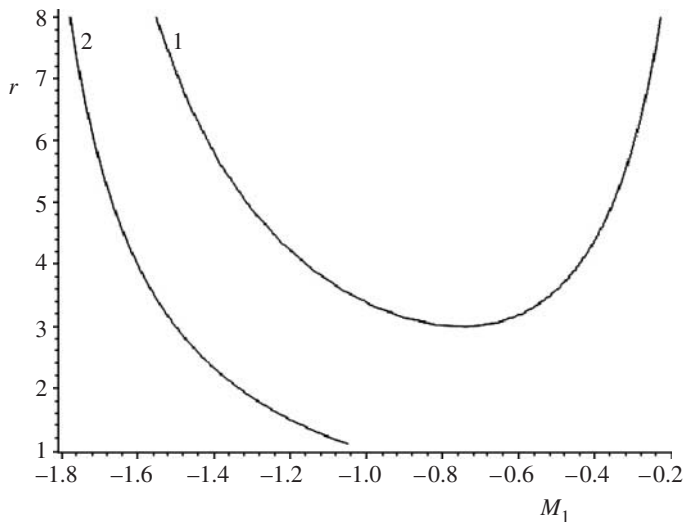


Figure 10. The case of the zero total mass perturbation ($M_1 + M_2 = 0$) corresponding to the extremal localization. (1) The optimal contrast parameter $r = m_1 + m_2$ versus the perturbation mass M_1 . (2) The lower bound for the admissible values of the perturbation mass M_1 .

for lattices of different contrasts. The graphs are given for the cases when ($r=1.2, 2, 3, 5$). It appears that for a sufficiently high contrast ($r \geq 3$), the extremal localization can be achieved via a perturbation whose total mass $M_1 + M_2$ is equal to zero. The special case of the zero total mass perturbation ($M_1 + M_2 = 0$) is illustrated in figure 10. For the case of the extremal localization, we show the lattice contrast parameter $r = m_1/m_2$ as a function of the perturbation mass M_1 . The curve on the left shows the lower boundary for the admissible values of the perturbation mass M_1 .

(c) *The frequency exceeds the upper bound*

For the two-mass chain, in addition to the above-considered band gap, no sinusoidal wave exists if $\Omega > \Omega_{\max} = 2/m_1 + 2/m_2 = 2 + r + 1/r$. For this case we find from equation (5.7) that

$$\begin{aligned} u_{1,m} &= \frac{1}{\sqrt{Q_0^2 - 4Q_0}} \{[-P_1(m_2\Omega - 2) + P_2]\lambda^{|m|} + P_2\lambda^{|m-1|}\}, \\ u_{2,m} &= \frac{1}{\sqrt{Q_0^2 - 4Q_0}} \{[-P_2(m_1\Omega - 2) + P_1]\lambda^{|m|} + P_1\lambda^{|m+1|}\} \quad \text{and} \\ 0 < \lambda &= \frac{1}{2} \left(Q_0 - 2 - \sqrt{Q_0^2 - 4Q_0} \right) < 1 \quad \left(\frac{2}{m_1} + \frac{2}{m_2} < \Omega \right). \end{aligned} \quad (5.15)$$

In particular,

$$\begin{aligned} u_{1,0} &= \frac{-P_1(m_2\Omega - 2) + (1/2)P_2 \left(Q_0 - \sqrt{Q_0^2 - 4Q_0} \right)}{\sqrt{Q_0^2 - 4Q_0}}, \\ u_{2,0} &= \frac{-P_2(m_1\Omega - 2) + (1/2)P_1 \left(Q_0 - \sqrt{Q_0^2 - 4Q_0} \right)}{\sqrt{Q_0^2 - 4Q_0}}, \\ Q_0 &= (m_1\Omega - 2)(m_2\Omega - 2) > 0 \quad \left(\frac{2}{m_1} + \frac{2}{m_2} < \Omega \right). \end{aligned} \quad (5.16)$$

Replacing $P_1 = M_1\Omega u_1$, $P_2 = M_2\Omega u_2$ we derive a system of two linear equations with respect to u_1 and u_2 , which has a non-trivial solution if and only if

$$\begin{aligned} &\left(\sqrt{Q_0^2 - 4Q_0} + M_1\Omega(m_2\Omega - 2) \right) \left(\sqrt{Q_0^2 - 4Q_0} + M_2\Omega(m_1\Omega - 2) \right) \\ &- \frac{M_1M_2\omega^4}{4} \left(Q_0 - \sqrt{Q_0^2 - 4Q_0} \right)^2 = 0 \quad \left(\Omega > \frac{2}{m_1} + \frac{2}{m_2} = \frac{(1+r)^2}{r} \right). \end{aligned} \quad (5.17)$$

From this it follows that, for any frequency in the infinite band gap, the localized oscillation state can be achieved by an allowable variation of each mass, e.g. $m_1 \rightarrow m_1 + M_1 > 0$ ($M_2 = 0$) or $m_2 \rightarrow m_2 + M_2 > 0$ ($M_1 = 0$)

$$\begin{aligned} M_1 &= -\frac{1}{\Omega} \sqrt{\frac{m_1\Omega - 2}{m_2\Omega - 2}} \sqrt{Q_0 - 4} > -m_1 \quad (M_1 < 0, M_2 = 0) \quad \text{and} \\ M_2 &= -\frac{1}{\Omega} \sqrt{\frac{m_2\Omega - 2}{m_1\Omega - 2}} \sqrt{Q_0 - 4} > -m_2 \quad (M_2 < 0, M_1 = 0). \end{aligned} \quad (5.18)$$

6. Concluding remarks

The localized vibration modes considered in this paper are described within the general analytical framework. The motivation of the paper is twofold: *first*, we discuss constructive ways to design band gap materials, both in the continuous case and in the case of discrete lattice structures and; *second*, we develop analytical descriptions of localized vibration modes within unbounded solids or lattices.

Although some of the formulations may look fairly classical, the analysis has generated new results not published elsewhere. For example, we have considered a uniform continuous configuration (including a ‘non-local’ material), which possesses a band gap for high frequencies; for this case, a high-frequency localized vibration mode is constructed and analysed. Analytical description and closed-form asymptotes have been derived for lattice Green’s functions characterizing high-frequency vibrations within the lattice and hence possessing an exponential decay at infinity.

The notions of the depth of band gaps and the localization exponents are used for the band gap structures, which possess localized vibration modes. We have presented the analysis of complex dispersion relations and ‘exponential waves’.

Finally, we have addressed a class of problems of optimal design for inhomogeneous lattice structures. By placing a frequency of the vibration mode within the band gap, we show the way to choose the physical parameters of the system to achieve the extremal localization. In particular, this can be achieved by a perturbation of a central cell within an inhomogeneous periodic lattice. It is also shown that a ‘neutral’ perturbation (which does not alter the total mass of the central cell) may be introduced for a certain class of lattices in such a way that the corresponding vibration mode is characterized by the extremal localization.

This paper has been written during the academic visit of Prof. Slepyan to Liverpool University supported by the research grant EP/D079489/1 from the UK Engineering and Physical Sciences Research Council. The authors acknowledge stimulating discussions with Prof. R. C. McPhedran following his lecture on defect modes in photonic crystal structures.

References

- Bacon, M. D., Dean, P. & Martin, J. L. 1962 Defect modes in two-component chains. *Proc. Phys. Soc.* **80**, 174–189. (doi:10.1088/0370-1328/80/1/321)
- Brillouin, L. 1953 *Wave propagation in periodic structures*. New York, NY: Dover.
- Cai, C. W., Liu, J. K. & Yang, Y. 2005 Exact analysis of localized modes in two-dimensional bi-periodic mass-spring systems with a single disorder. *J. Sound Vib.* **288**, 307–320. (doi:10.1016/j.jsv.2005.01.044)
- Callaway, J. 1964 Theory of scattering in solids. *J. Math. Phys.* **5**, 783–798. (doi:10.1063/1.1704180)
- Gazis, D. C. & Wallis, R. F. 1964 Surface tension and surface modes in semi-infinite lattices. *Surface Sci.* **3**, 19–32.
- John, S. 1987 Strong localization of Photons in certain disordered dielectric superlattices. *Phys. Rev. Lett.* **58**, 2486–2489. (doi:10.1103/PhysRevLett.58.2486)

- Jensen, J. S. 2003 Phononic band gaps and vibrations in one- and two-dimensional mass–spring structures. *J Sound Vib.* **226**, 1053–1078. (doi:10.1016/S0022-460X(02)01629-2)
- Langley, R. S. 1996 The response of two-dimensional periodic structures to point harmonic forcing. *J Sound Vib.* **197**, 447–469. (doi:10.1006/jsvi.1996.0542)
- Langley, R. S. 1997 The response of two-dimensional periodic structures to impulsive point loading. *J Sound Vib.* **201**, 235–253. (doi:10.1006/jsvi.1996.0744)
- Langley, R. S., Bardell, N. S. & Ruivo, H. M. 1997 The response of two-dimensional periodic structures to harmonic point loading: a theoretical and experimental study of a beam grillage. *J. Sound Vib.* **207**, 521–535. (doi:10.1006/jsvi.1997.1154)
- Maradudin, A. A., Montroll, E. W. & Weiss, G. H. 1963 *Theory of lattice dynamics in the harmonic approximation*. New York, NY: Academic Press.
- Maradudin, A. A. 1965 Some effects of point defects on the vibrations of crystal lattices. *Rep. Prog. Phys.* **28**, 332–380. (doi:10.1088/0034-4885/28/1/310)
- Martin, P. A. 2006 Discrete scattering theory: Green's function for a square lattice. *Wave Motion* **43**, 619–629. (doi:10.1016/j.wavemoti.2006.05.006)
- Martinsson, P. G. & Movchan, A. B. 2003 Vibrations of lattice structures and phononic band gaps. *Q. J. Mech. Appl. Math.* **56**, 45–64. (doi:10.1093/qjmam/56.1.45)
- Mead, D. J. 1973 A general theory of harmonic wave propagation in linear periodic systems with multiple coupling. *J Sound Vib.* **27**, 235–260. (doi:10.1016/0022-460X(73)90064-3)
- Mead, D. J. 1996 Wave propagation in continuous periodic structures: research contributions from Southampton, 1964–1995. *J. Sound Vib.* **190**, 495–524. (doi:10.1006/jsvi.1996.0076)
- Mead, D. J. & Parthan, S. 1979 Free wave propagation in two-dimensional periodic plates. *J. Sound Vib.* **64**, 325–348. (doi:10.1016/0022-460X(79)90581-9)
- Mead, D. J. & Yaman, Y. 1991 The harmonic response of rectangular sandwich plates with multiply stiffening a flexural wave analysis. *J. Sound Vib.* **145**, 409–428. (doi:10.1016/0022-460X(91)90111-V)
- Morita, T. & Horiguchi, T. 1972 Lattice Green's function for the diatomic lattices. *J. Math. Phys.* **13**, 1243–1252. (doi:10.1063/1.1666129)
- Poulton, C. G., McPhedran, R. C., Nicorovici, N. A. & Botten, L. C. 2003 Localized Green's functions for a two-dimensional periodic material. In *IUTAM Symp. on Asymptotics, Singularities and Homogenisation in Problems of Mechanics* (ed. A. B. Movchan), pp. 181–190. Dordrecht, The Netherlands: Kluwer.
- Slepyan, L. I. & Ayzenberg-Stepanenko, M. Submitted. Resonant-frequency primitive waveforms and star waves in lattices.
- Yablonovitch, E. 1987 Inhibited spontaneous emission in solid-state physics and electronics. *Phys. Rev. Lett.* **58**, 2059–2062. (doi:10.1103/PhysRevLett.58.2059)
- Yablonovitch, E. 1993 Photonic band-gap crystals. *J. Phys. Condensed Matter* **5**, 2443–2460. (doi:10.1088/0953-8984/5/16/004)